THE OPTICAL BIREFRINGENCE STUDY OF [4-(4-CHLOROBENZYLOXY)-3-METHYLPHENYL](*p*-TOLYL)DIAZENE DYE

Vily Marius CIMPOIAŞU[1], Ion PĂLĂRIE[2], George BRĂTULESCU[3], Constanta DASCĂLU[4], Petre ROTARU[5]

We report an extension of experimental technique (version of the Chang method) for the measurement of the optical birefringence of [4-(4-chlorobenzyloxy)-3-methylphenyl](p-tolyl)diazene dye in NLC phase. The azo dye shows birefringence only for cooling cycle, due to the increasing of molecular order by hydrogen bond associations. We create an extension from three-band model to four-band model and estimate the dispersion of optical birefringence $\Delta n(\lambda,T)$ by applying a nonlinear fitting procedure on the rescaled transmittance $Tr(\lambda,T)$. We obtained the parameters $G_0(T)$, $G_1(T)$, $G_2(T)$, $G_3(T)$ involved in the calculation of $\Delta n(\lambda,T)$. We use interference to accurate measure of temperature dependence of cell thickness D(T). The most important band involved in birefringence was λ_0~120 nm, followed by λ_3~369 nm, while λ_1~258 nm and λ_2~340nm bands were not important.

Keywords: optical birefringence, azo dye, nematic liquid crystal.

1. Introduction

Nematic liquid crystals (NLCs) are known to behave locally as uniaxial anisotropic media. Their optical birefringence, Δn, is high, ($\Delta n = n_E - n_o \sim 0.2$) and can be modified by varying the temperature and / or the external field. n_E is the principal extraordinary refractive index, so it corresponds to a polarization of the light beam parallel to the optical axis, while n_o is the ordinary refractive index, related with a polarization of the light beam orthogonal to the optical axis.
The physical origin of liquid crystal refractive index dispersion's has been investigated in many papers [1-4]. The three-band model is a usual model, which explains the experimental data very well [3-4]. As an extension of three-band model, we propose a larger model (four-band model), consist by a single σ-σ*

[1] Dept. of Physics, Prof., Dept. of Biology and Environmental Engineering, University of Craiova, Romania, e-mail: vilycimpoiasu@yahoo.com,
[2] Lecturer, Dept. of Physics, University of Craiova, Romania, corresponding author, e-mail: palarie_i@yahoo.com,
[3] Prof., Dept. of Chemistry, University of Craiova, georgebratulescu@yahoo.com,
[4]Assoc. Prof., Dept. of Physics, University POLITEHNICA of Bucharest, Romania, e-mail: dascaluc@yahoo.com,
[5]Prof., Dept. of Physics, University of Craiova, Romania, e-mail: petrerotaru@yahoo.com.

transition (designated as the λ_0-band, located in the vacuum UV region, λ_0~ 120nm) and three π-π^* transitions (designated as the λ_1, λ_2 and λ_3-bands, with $\lambda_3 > \lambda_2 > \lambda_1$ placed in the nearby ultraviolet and obtained by using the absorption spectrum of the liquid crystal under study).

For this model, in the visible and infrared regions, $\Delta n(\lambda,T)$ are:

$$\Delta n(\lambda,T) = \frac{G_0(T)}{\left(1/\lambda_0^2 - 1/\lambda^2\right)} + \frac{G_1(T)}{\left(1/\lambda_1^2 - 1/\lambda^2\right)} + \frac{G_2(T)}{\left(1/\lambda_2^2 - 1/\lambda^2\right)} + \frac{G_3(T)}{\left(1/\lambda_3^2 - 1/\lambda^2\right)} \quad (1)$$

where λ is the wavelength of light, T the temperature of the NLC and $G_0(T)$, $G_1(T)$, $G_2(T)$, $G_3(T)$ represent parameters which are temperature-dependent [3].

In this paper we present an experimental technique based on extended model. The oriented planar nematic layer is observed in a beam of white light (LS-1-LL Tungsten Halogen light source). NLC is placed between parallel/perpendicular polarizers, while an angle of 45^o is maintain between the optical axis of NLC and polarizers. The light intensity transmitted by the analyzer $I_t(\lambda,T)$ depends on wavelength and was recorded at different temperatures (113-119 ^{o}C) within the nematic phase range of NLC. To calculate the birefringence $\Delta n(\lambda,T)$, we estimate the characteristic band parameters ($G_0(T)$, $G_1(T)$, $G_2(T)$, $G_3(T)$) by using a non-linear fitting procedure of the recorded light intensity $I_t(\lambda,T)$ [5]. This simplest experimental method allow us to measure locally the sample cell by using fine optic fibers. Our method use a spectrometer connected to a computer for recording experimental data, in opposition with other methods (modified Talbot-Rayleigh method [6] record the channeled spectra by requiring a diffraction grating, a linear CCD matrix, which must be calibrated by using interference filters).

2. Structural formula, absorption spectrum and nematic phase range of [4-(4-chlorobenzyloxy)-3-methylphenyl](*p*-tolyl)diazene

The azo dye [4-(4-chlorobenzyloxy)-3-methylphenyl](*p*-tolyl)diazene has been synthesized [7] and studied from the point of view of the chemical kinetics and thermal analysis [8]. Its structural formula is given in Figure 6A.

The UV absorption spectrum (Fig. 1) of [4-(4-chlorobenzyloxy)-3-methylphenyl](*p*-tolyl)diazene solution in 1,4-dioxane solvent was obtained with an Ocean Optics Spectrometer HR4000. We use 1,4-dioxane solvent because is UV transparent. We remark the four absorption bands, three in UV range, λ_1= 258.93 nm, λ_2 = 340.13 nm, λ_3 = 369.06 nm and one in visible range λ_4 = 444.84 nm.

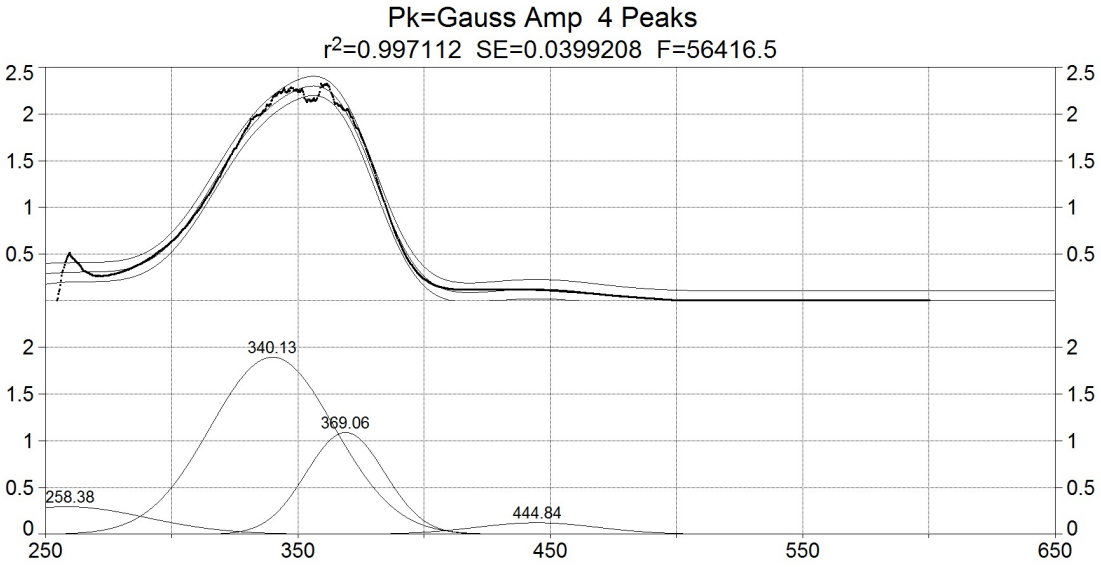

Fig. 1. Absorption spectrum of [4-(4-chlorobenzyloxy)-3-methylphenyl](*p*-tolyl)diazene in 1,4-dioxane.

3. Cell design and properties

In all measurements we use a standard sandwich glass cell. A solution of polyvinyl alcohol (PVA) and water (3:100) was spin coated on the inner surfaces of the glasses (at room temperature and 2000 rot/min [9]). The resulting thin polymeric film with a thickness ~100nm [9] has been baked for one hour in an oven at 120°C to provide full polymerization of PVA. Next, the thin film has been rubbed along a given direction to create support structure for planar alignment of the NLC along the rubbing direction. The glass plates of the cell have been distanced at about 23 μm by using Mylar spacers and sealed together by high temperature flexible epoxy resin.

In the next phase, we fill the cell with [4-(4-chlorobenzyloxy)-3-methylphenyl](*p*-tolyl)diazene by capillarity at temperature higher than 137.3°C (clarification point). The cell was not fill completely and transparent portion of cell was use for accurate determination of cell thickness at various temperatures.

The critical parameter in accurate determination of birefringence is cell thickness D (the distance between the inner faces of the cell plates). The experimental setup used is presented in Fig. 2, with parallel configuration of polarizer 10 and analyzer 11. To determine D, we have recorded the wavelength dependence of the interference of light, transmitted by the empty portion of cell.

The LS-1-LL Tungsten Halogen light source (7) provide a good spectral range (360-2000nm). The parallel beam from the optical fiber+convergent lens

(6A) emerges at normal incidence on the cell and transmitted light go to Ocean Optics Spectrometer HR4000 (8) through the optical fiber (6B). The computer (9) records the wavelength-dependent transmitted intensity of the empty portion of the cell (we present in Fig. 3 only 500-1000nm range).

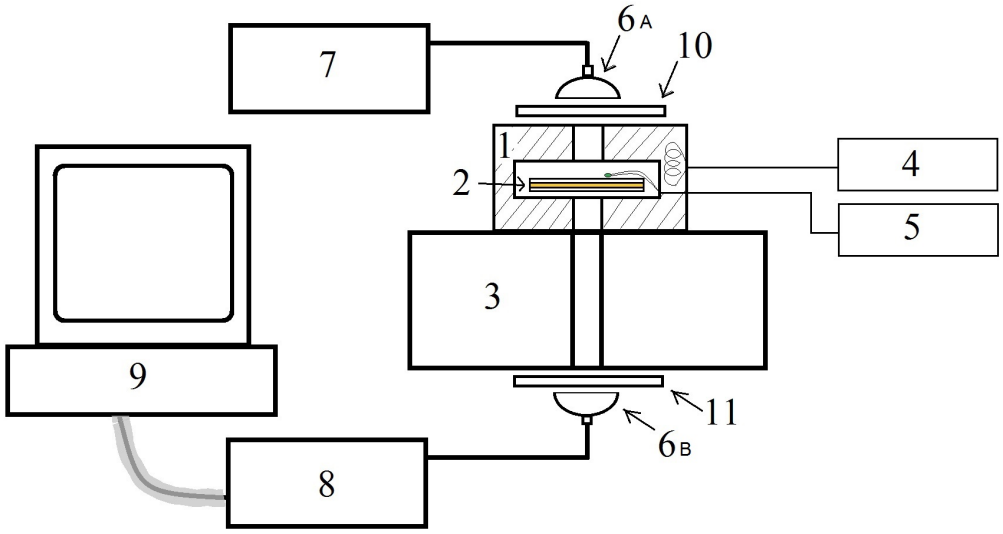

Fig. 2. The cell filled with substance is placed inside a home made special electric oven (1), connected with a temperature controller unit (4) that allow us to cool and heat the sample with linear temperature rate (1-3°C/min). The temperature was measured with a Constantan-Copper thermocouple connected to a KEITHLEY 2000 multimeter of 0.01°C precision (5). The oven is placed on the table (3) of an IOR-MC5A microscope for proper align of cell. Fine optical fiber + convergent lens (6A) provide parallel light beam normal on the cell and optical fiber + convergent lens (6B) transmit light beam to spectrometer (8) OCEAN Optics UV-VIS HR4000, controlled by the computer (9). (10) Polarizer and (11) Analyzer.

The connection between D, the wavelength of the light (λ), and the K_{max}-th interference order at maximum (respective minimum K_{min}) transmission is:

$$K_{max}=\frac{2D}{\lambda}, K_{min}=\frac{2D}{\lambda}+\frac{1}{2}, \tag{2}$$

which indicates a linear dependence between K_{max} (respective K_{min}-1/2) on 1/λ.

We obtain the slope B=2D from linear dependence K= A+B·(1/λ). With a suitable choice of interference order for both minimum and maximum, A goes to zero, while the value of B is independent from it (Fig. 4).

The thickness of the cell (D~23 μm) has been computed for many cell temperatures (see Fig. 5). The interpolated curve shows complex behavior (step function). This temperature feature is justified by complex phase transitions of the azo dye (isotropic liquid → NLC→ crystal) [8,10]. For birefringence measurements we use estimated value (red curve) for cell thickness.

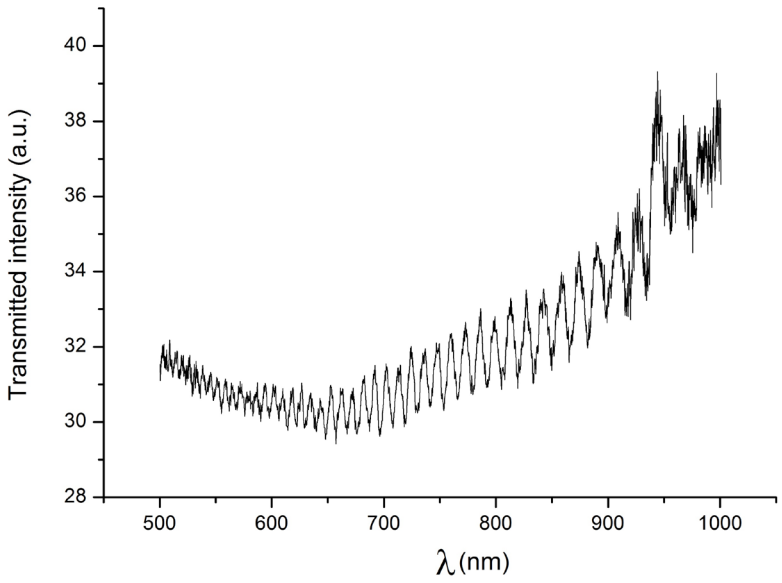

Fig. 3. Transmitted light intensity for transparent portion of cell.

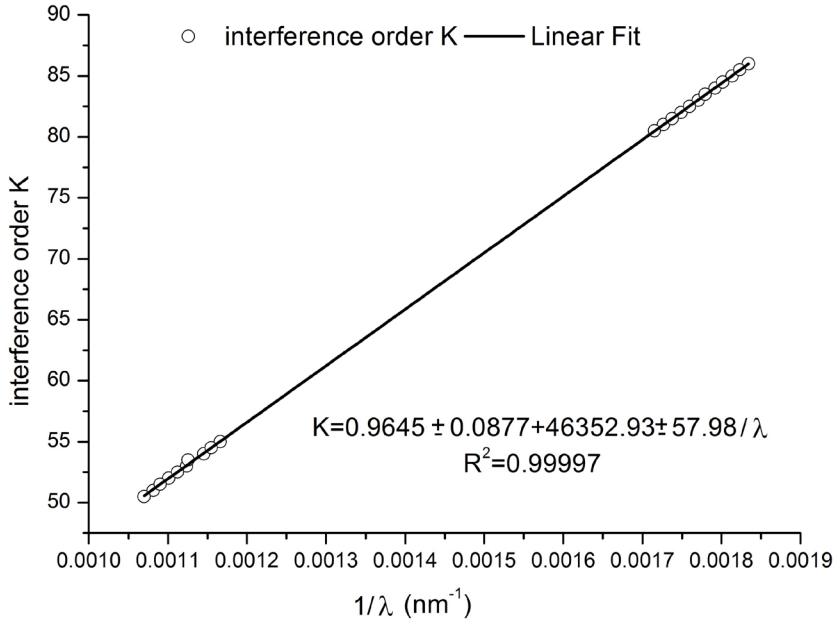

Fig. 4. Linear dependence of the interference order K on inverse λ . We chose 11 value for K_{max} and 11 values for K_{min} at the both ends of the spectral interval range.

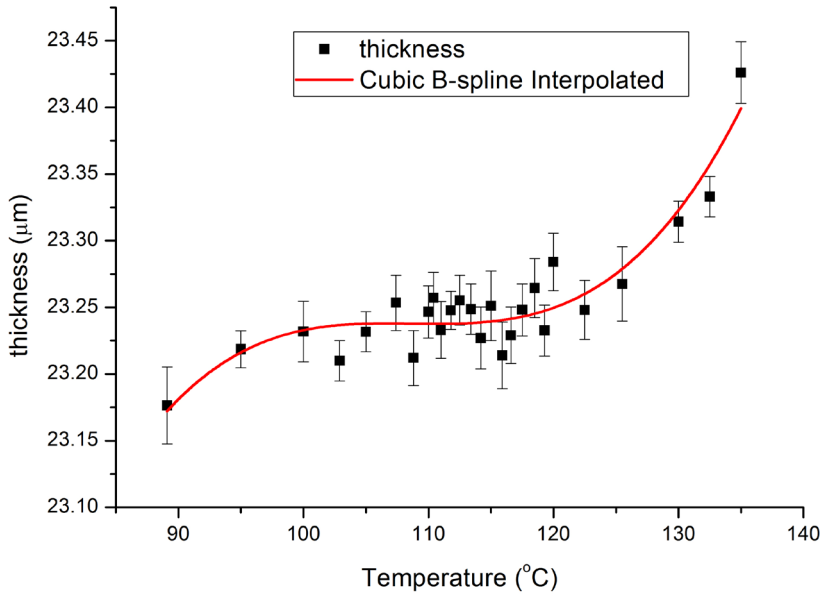

Fig. 5. Temperature dependence of cell thickness D.

4. Birefringence measurements

Next, we center the white light beam on the filled portion of cell by move the cell inside oven.

The nematic range was previously determined by G. Brătulescu and published in 1996, in the first cotutelle doctoral thesis [10] in Romania and France. Experimentally we found nematic range 118.5-113.5°C that it is in good accordance with the theoretical range 119.5-116.8 °C [10].

We perform heating and next cooling cycles from 90→155→ 90°C (not very fast, 1-3°C/min), waiting for the appearance of grooved figures, specific for birefringence (see Fig. 8). First we observe that only at cooling appear the birefringence figures.

The possible explanation is given in the next paragraphs.

The hydroxyl groups on the surface of the polyvinyl alcohol form hydrogen bonds with the atoms of the azo group -N=N- and of the etheric group -OCH_2-. These bonds are accomplished with the help of electron pairs from nitrogen and oxygen atoms.

The hydrogen bond is stronger with the azo group due to the higher basic character of the sp^2 hybridized nitrogen atom. On the other hand, a resonant structure (B from Fig. 6) can be written on the molecule of the compound (A) in which a negative charge is observed at the first nitrogen atom.

Therefore, the liquid crystal molecules interact with the polyvinyl alcohol located on the inner faces of the glass cell, the lower and upper, in which the optical measurements were performed.

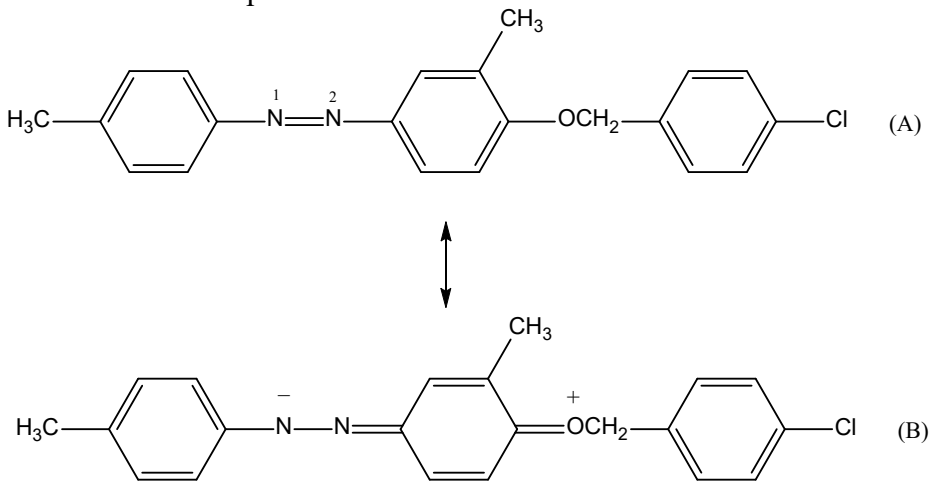

Fig. 6. Compound structure (A) and resonant compound structure (B).

The interaction consists in an association by hydrogen bonds between the first layer of molecules from the volume of liquid crystal and the polyvinyl alcohol molecules (see Fig. 7). The hydrogen bond interaction can be depicted as follows:

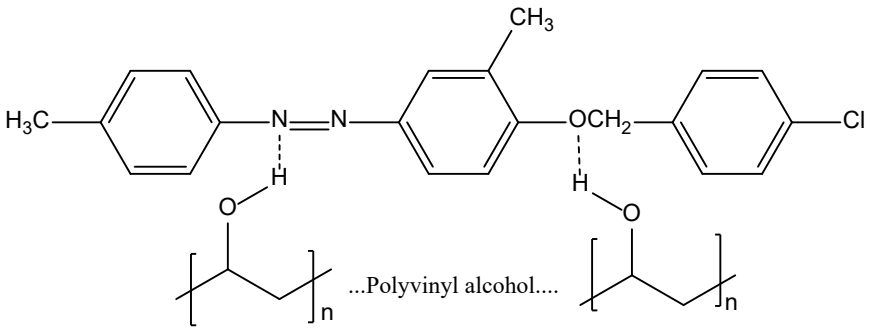

Fig. 7. Hydrogen bonds formations between compounds and PVA.

The strength of these hydrogen bonds is higher for the atoms of the azo group, where the electron density is higher, than for the atoms of the ether group. Hydrogen bonds are sensitive to temperature variation.

By heating the liquid crystal, near the melting point, due to thermal agitation, the hydrogen bonds are broken. First, the hydrogen bonds in the etheric group -OCH_2- break, followed by the hydrogen bonds in the azo group -N=N-. At this point the mobility of the liquid crystal molecules becomes maximum.

On the contrary, by cooling the compound from the melting point (isotropic liquid) to the liquid crystal phases, the hydrogen bond associations with

polyvinyl alcohol are restored: first, in the azo group –N=N–, then in the etheric group. Consequently, the molecular order (alignment) increases. Due to this behavior, there are different changes in the structure of the liquid crystal phases when heating and cooling the optical measurement cell, respectively.

The sample is maintained in the oven with the optical axis tilted at 45° to the perpendicular/parallel configuration of the polarizers. The transmitted light $I_t(\lambda,T)$ is recorded using the spectrometer at various temperatures only for cooling cycle within the nematic phase temperature range.

The recording procedure was extensively described in paper [5]. We extend the measurements using both configuration of polarizers, parallel and perpendicular.

The experimental transmittance (see Figure 8) was fitted conform with theoretical dependence:

$$Tr(\lambda,T) \equiv \frac{I_t(\lambda,T) - Dark(\lambda)}{I_I(\lambda) - Dark(\lambda)} \propto \sin^2\left[\frac{\pi * \Delta n(\lambda,T) * D(T)}{\lambda}\right]$$ for perpendicular,

$$Tr(\lambda,T) \equiv \frac{I_t(\lambda,T) - Dark(\lambda)}{I_I(\lambda) - Dark(\lambda)} \propto \cos^2\left[\frac{\pi * \Delta n(\lambda,T) * D(T)}{\lambda}\right]$$ for parallel,

where D(T) is thickness, $\Delta n(\lambda,T)$ is birefringence and $Dark(\lambda)$ is dark signal recorded without light source. $I_I(\lambda)$ represent the intensity in the absence of cell and parallel polarizers.

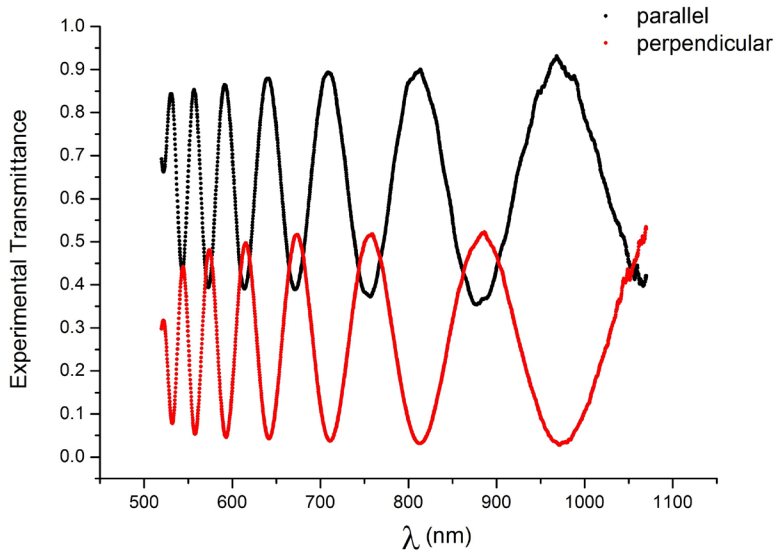

Fig. 8. Experimental transmittance of cell at 117.5°C for parallel/perpendicular configurations of polarizers.

For accurate extraction of birefringence parameters $G_0(T)$, $G_1(T)$, $G_2(T)$, $G_3(T)$, using a nonlinear fitting procedure [5,11] the experimental transmittance needs to be rescaled between 0 and 1 respectively. In Fig. 9 we present rescaled transmittance and fitting functions.

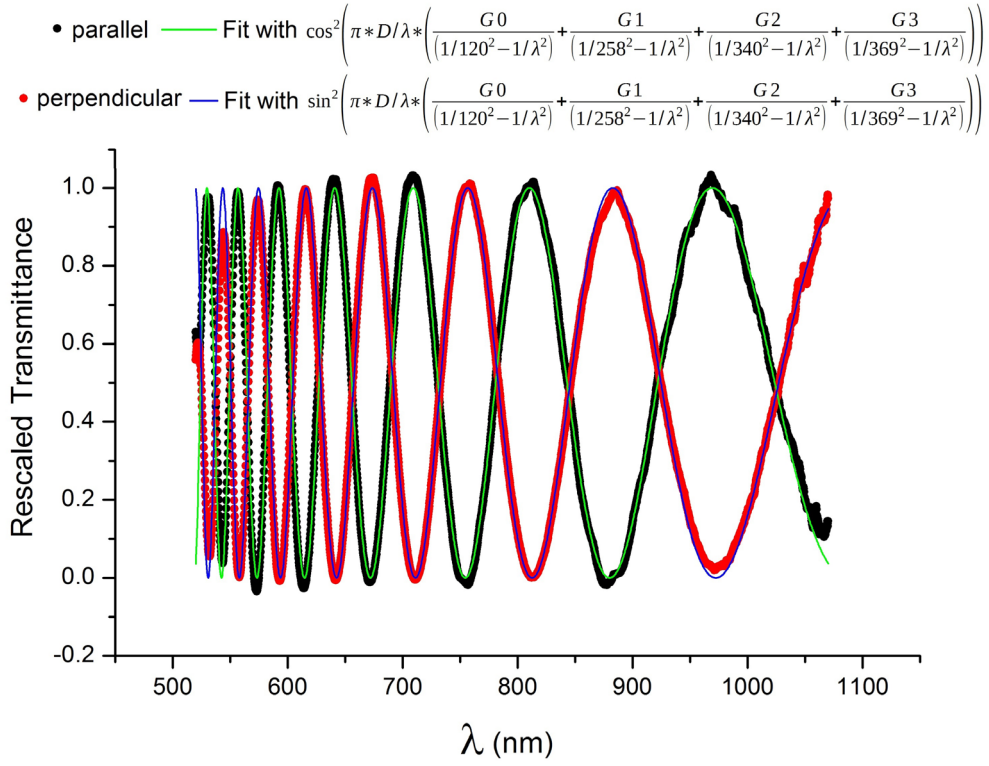

Fig. 9. Rescaled transmittance and fit functions of cell at 117.5°C for both configurations of polarizers, parallel/perpendicular.

The fitting procedure give good statistical results, the reduced χ^2 for all measurements is between $0.6 \cdot 10^{-4}$ and $1.8 \cdot 10^{-3}$.

The temperature dependence of band parameters $G_0(T)$, $G_1(T)$, $G_2(T)$, $G_3(T)$, represented in Figure 10, shows that the most important band involved in birefringence are $\lambda_0 \sim 120$nm and $\lambda_3 \sim 369$nm.

We obtain similar values for $G_0(T)$, and $G_3(T)$ in both configurations. The great dispersion of $G_1(T)$, and $G_2(T)$ parameters is due, in principle, to the very small values with tiny contributions in birefringence and instabilities of nonlinear mathematical procedure for fit. However, small contributions in birefringence of λ_1 and λ_2 bands are truly important. The optical birefringence $\Delta n(\lambda,T)$, calculated conform eq. 1 and represented in Fig. 11 exhibit a normal behavior with temperature.

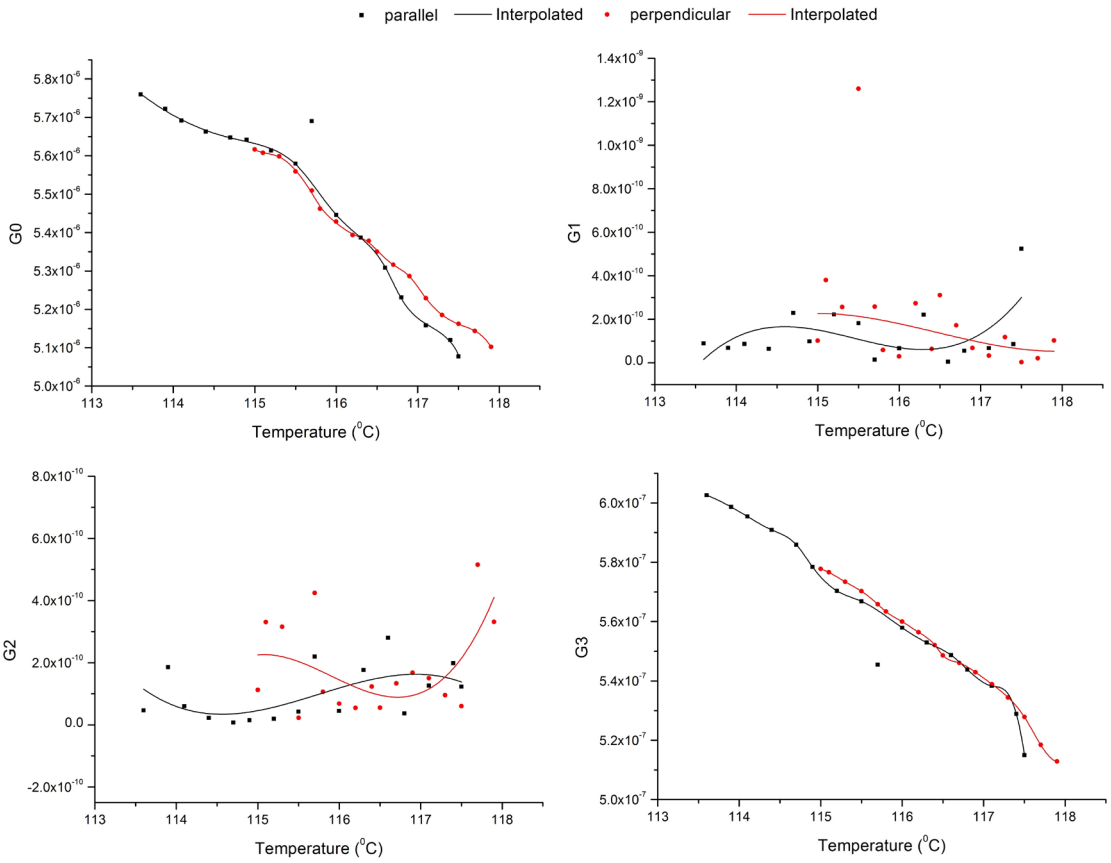

Fig. 10. The temperature dependence of band parameters $G_0(T)$, $G_1(T)$, $G_2(T)$, $G_3(T)$.

5. Conclusions

We found that azo dye [4-(4-chlorobenzyloxy)-3-methylphenyl](*p*-tolyl)diazene shows optical birefringence only for cooling cycle, due to the increasing of molecular order by hydrogen bond associations. To measure this, we have developed a new technique of processing experimental data where we essentially considered all the experimental data and the dispersion of optical birefringence $\Delta n(\lambda,T)$ in the framework of extension the three-band model to four-band model (using a version of the Chang method [12]).

In order to obtain an accurate nonlinear fitting procedure on the rescaled $Tr(\lambda,T)$ we first measure by interference the cell thickness $D(T)$ and second we evaluate the parameters $G_0(T)$, $G_1(T)$, $G_2(T)$, $G_3(T)$ involved in the calculation of $\Delta n(\lambda,T)$. The values of $\Delta n(\lambda,T)$ obtained there are in accordance with the ones reported in [13]. We conclude that the most important band involved in birefringence was λ_0~120nm, followed by λ_3~369nm, and other bands λ_1~258 nm and λ_2~340nm have insignificant contribution.

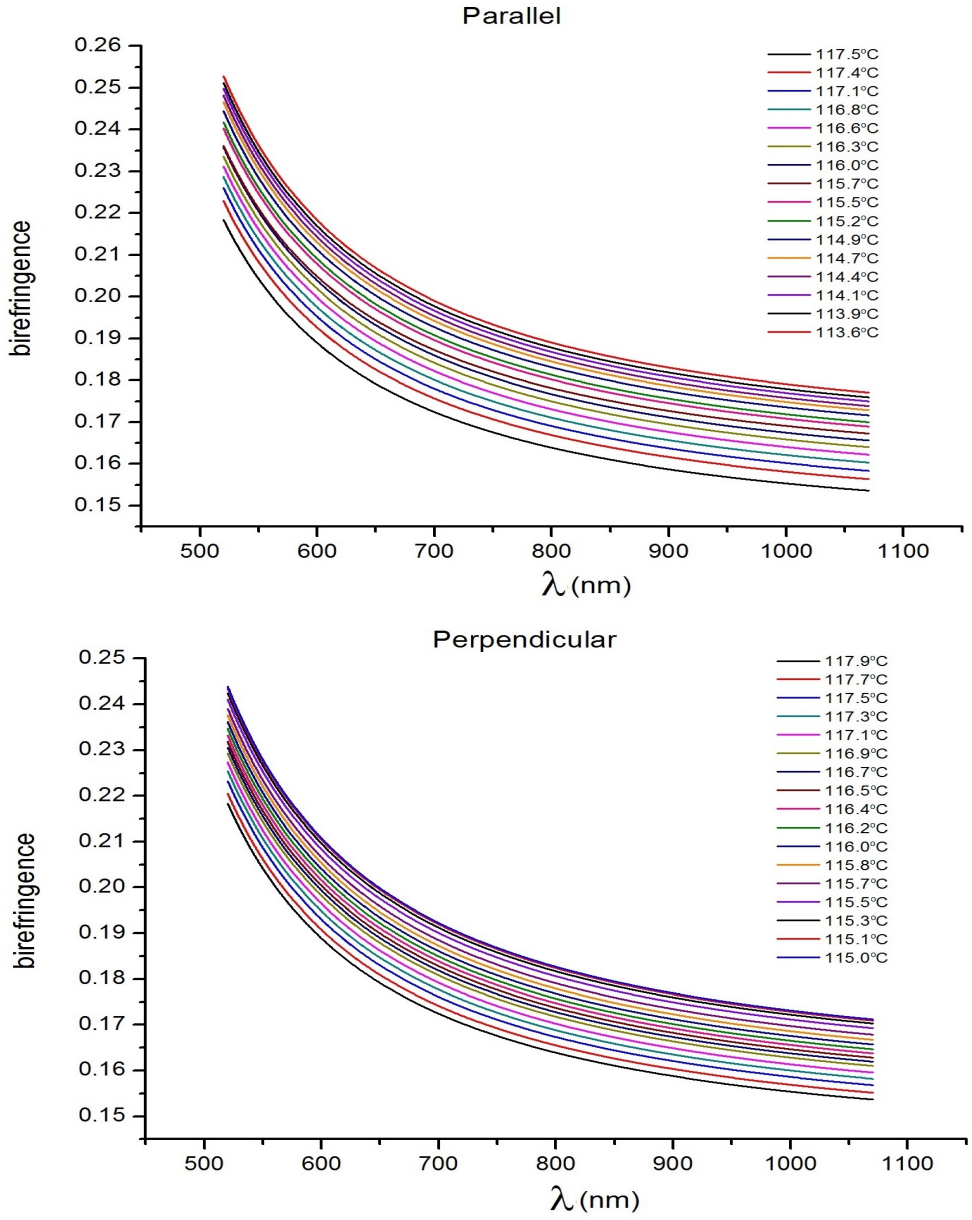

Fig. 11. The birefringence dispersion obtained by using both configurations at various temperatures.

REFERENCES

[1]. *M. F. Vuks*, "Determination of the optical anisotropy of aromatic molecules from the double refraction of crystals", in Opt. Spektrosk., **vol. 20**, 1966, pp. 644–647.

[2]. *S. T. Wu*, "Birefringence dispersions of liquid crystals", in Phys. Rev. A, **vol. 33**, no. 2, 1986, pp. 1270-1274.

[3]. *S. T. Wu*, "A semiempirical model for liquid-crystal refractive index dispersions", in J. Appl. Phys., **vol. 69**, no.4, 1991, pp. 2080-2087.
[4]. *S. T. Wu*, *C. S. Wu, M. Warenghem, M. Ismaili,* "Refractive index dispersion of liquid crystals", in Opt. Eng., **vol. 32**, no. 8, 1993, pp. 1775-1780.
[5]. *I. Palarie, M. Socaciu, M. Ursache, C. Florea,* "A new version of the Chang method for the determination of the optical birefringence of nematic liquid crystals", in Journal of Optoelectronics and Advanced Materials, **vol. 8**, no. 1, 2006, pp. 291-294.
[6]. *M. Socaciu, M. Ursache, "*Dispersion curves computed from channeled diffraction spectra of liquid crystals*",* in Mol. Cryst. Liq. Cryst., **vol. 403**, 2003, pp. 1-13.
[7]. *G. Brătulescu, Y. Le Bigot, M. Delmas*,"Use of electromagnetic micro-waves without solvent or absorbent support: application to the synthesis of aromatic azoethers", in Synthetic Commun., **vol. 27**, 1997, pp. 1037–1042.
[8]. *A. Rotaru, G. Brătulescu, P. Rotaru*, "Thermal analysis of azoic dyes: Part I. Non-isothermal decomposition kinetics of [4-(4-chlorobenzyloxy)-3-methylphenyl](p-tolyl)diazene in dynamic air atmosphere", in Thermochimica Acta, **vol. 489**, 2009, pp. 63–69.
[9]. *J. Cognard*, Alignment of Nematic Liquid Crystals and their Mixtures, Gordon & Breach Sci. Publ., New York, 1982.
[10]. *G. Brătulescu,* Synthèse d'azoéthers aromatiques par réaction de Williamson réalisée en milieu homogène et en milieux hétérogènes: solide-liquide, liquide-liquide et sous l'action de micro-ondes électromagnétiques, PhD Thesis, UPB Bucharest (Romania) & Institut National Polytechnique de Toulouse (France), 1996.
[11]. *I. Palarie, C. Florea*,"Refractive indices determination of a new nematic liquid crystal", in Journal of Optoelectronics and Advanced Materials, **vol. 7**, no. 2, 2005, pp. 997-1007.
[12]. *R. Chang,* "The Anisotropic Refractive Indices Of Mbba", in Mol. Cryst. Liq. Cryst., **vol. 34**, 1976, pp. 65-69.
[13]. *K. Thingujam, A. Bhattacharjee, B. Choudhury, R. Dabrowski*,"Nematic liquid crystals exhibiting high birefringence", in Optical Review, **vol. 23**, no. 3, 2016, pp. 409-419.